DIRC Note #129

April 12, 2000

Internal Group Note

Quartz absolute internal reflection coefficient, water transmission, mirror reflectivity, mean wavelength response, mean refraction index, and their effect on the expected number of photoelectrons and N_o.

J. Va'vra

Abstract

This note presents results of my lab measurements of the wavelength dependency of the absolute value of the internal reflection coefficient, the absolute value of the water transparency during the first year of BaBar physics running, the reflectivity of mirrors and various candidates for the shim material. I also estimate expected number of photoelectrons, mean Cherenkov angle, mean refraction index, and the absolute value of N_o for three angles of incidence of 0°, +60°, and –60°.

1. The wavelength dependence of the internal reflection coefficient.

It is important to point out that the presented measurement in this paper is the absolute measurement of the internal reflection coefficient [1], i.e., no reference bar was used to normalize the results.

Boeing bar #114 is used for this measurement. The bar is 1.2247 m long, 3.495 cm wide and 1.646 cm thick. The internal reflection coefficient was measured on wide surfaces of the bar. Prior to this measurement, the bar surfaces were cleaned with the DIRC Group alumina powder technique (see discussion later) making sure that the surface chemical pollution is minimized. It was absolutely essential to do the cleaning to achieve the ultimate results. A randomly picked bar, which was not a subject to either the "alumina powder" cleaning or the regular "acetone/alcohol" DIRC cleaning procedures, could have had the reflection coefficient lower easily by ~0.0005. During the DIRC construction, we monitored the bar cleanliness carefully by the relative measurements of the reflection coefficient [2,3], where the bar#114 played a crucial role of the reference bar. Therefore, this note is important for providing the absolute normalization for all these measurements.

To measure the wavelength dependency, I used five laser wavelengths: 266, 325, 442, 543 and 633 nm. They were provided by four different lasers: Nanolase solid state YAG laser (266 nm), Lyconix He-Cd 4210N (325 or 442 nm), Uniphase 1135 red (543 nm) and Uniphase green (633 nm). The intensity of the lasers varies, which influences the relative accuracy for each measurement (for example, the Hamamatsu photodiode currents were ~500-600 μA at 442 nm, ~20-25 μA at 325 nm, ~10-15 μA at 266 nm, ~20-25 μA at 543 nm and ~500-550 μA at 633 nm). Similarly, laser stability varied, making the 266 nm Nanolase the least stable one.

The internal reflection coefficient was one of the parameters not measured directly for a long time in the DIRC group. One could adopt a complicated method, which assumes a complete optical analysis, including measurements of the entrance and exit angles. However, H. Krueger and J. Va'vra have invented much more simple method, called the "calorimetric" method [1]. This method simply measures five light intensities (see Fig. 1), the number of light bounces, and uses bar dimensions, i.e., no entrance or exit laser light angles are present in the problem. The internal reflection coefficient is measured absolutely with this technique. The starting equation is:

$$(((I_0 - I_1)r^N - I_2)r^N - I_3)r^N = I_4 \tag{1}$$

which in turn leads to:

$$I_0 = I_1 + I_2 * x + I_3 * x^2 + I_4 * x^3 \tag{2}$$

Its solution X is related to the coefficient of internal reflection r through the following equation:

This material is based upon work supported by the U.S. Department of Energy, Office of Science, under Contract No. DE-AC02-76SF00515.

$$x^{-1} = r^N * \exp\{-\frac{L}{\lambda} * \sqrt{[1+(\frac{bN}{L})^2]}\} \quad , \tag{3}$$

$$= (\text{Reflection\_coeff.})^N * \text{Transmission\_coeff.},$$

where N is the number of bounces, L is the length of the quartz bar, b is the width of the quartz bar, λ is the quartz attenuation length, and I_i the laser intensities. The laser setup was arranged to have N = 54 bounces at 442 nm. The quartz attenuation length λ is not an easy quantity to measure at long wavelengths using such a short bar (1.2 m long). After several experimental tests, I decided to use J. Schwiening's measurement [2] of the attenuation length of $\lambda = 499.5 \pm 167$ m at 442 nm, which is more accurate, because it was done with a computer controlled setup. For any other wavelength, I then scaled the attenuation length according to $1/\lambda^4$, assuming the Rayleigh's law. For example, this dependence gives λ ~2100 m at 633 nm, which would be impossible to measure using a ~1.2 m long bar with a good accuracy.

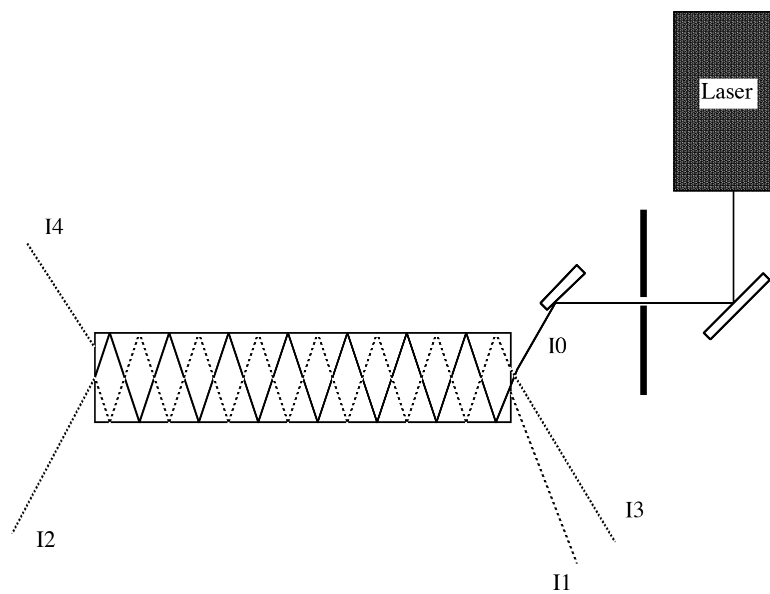

Figure 1. A schematic layout of the experiment to measure the reflection coefficient.

The DIRC Note #40 also describes further improvements in accuracy, by adding another term in equation (2), which can be calculated from the measured intensities by integrating higher order contributions (this improvement is credited to H. Kawahara):

$$I_0 = I_1 + I_2 * x + I_3 * x^2 + I_4 * x^3 + I_5 \tag{4}$$

where

$$I_5 = \frac{I_3^{\,3}}{I_2 * (I_2 - I_3)} \tag{5}$$

To do this part, I used the "Mathematica" program to solve the cubic equation (5), and the results were then used for the spreadsheet calculations. This correction increased the coefficient typically by ~0.0003.

Another small improvement in the accuracy, introduced by J. Schwiening and X. Sarazin, and described in DIRC Note #40, was a correction for a photodiode response due to the finite size of the laser beam. As the beam size for each intensity I_i changes, the correction is different for each I_i component. These corrections vary from 1.006 (I_{in} and I_o) to

1.03 (I_4). DIRC Note #40 quotes the measurement of these corrections at 325 and 442 nm wavelengths, respectively. Given the relatively small variation, I used the same corrections at the nearest laser wavelengths.

A factor in the precision of this measurement was a background light in the room, which can influence the weak reflection components such as I_3 or I_4. The effect of the background light was to increase the reflection coefficient. The solution was to work in the semi -dark conditions during the measurement.

There is also a question if the reflection coefficient varies depending which bar side is selected for the laser light reflection. All measurements quoted in this paper are based on the laser reflecting from the wide sides, although the calibration, based on the bouncing from the narrow sides, was also provided for Ref. 3.

The reflection coefficient dependency on the loss of light intensity due to the quartz lobe effect [4], which is caused by a slight modulation of the quartz refraction index, was not studied in this work. This effect could occur at some laser angle orientations relative to the bar axis. Making sure that the escaping laser beams do not have small lobes checked this particular systematic error. In addition, one does not expect a large effect for this type of quartz[1].

Finally, as we already mentioned, it was very important to clean the bars before this measurement to get the ultimate value of the reflection coefficient. We have developed a method to clean the surface with a mixture of distilled water and alumina powder. To ensure that it does not scratches the surface, we performed several tests described in Fig. 2, which shows the effect of cleaning with a 0.3 μm size alumina powder, mixed with the clean water with a ratio 1:10. We have used the 2-nd method, shown in Fig. 2, i.e., the rms surface finish remained at ~4 Å after the cleaning was finished. D. Millican and the author performed these tests. Incidentally, this particular cleaning method was also used for a small number of DIRC quartz bars (when the regular "acetone/alcohol" cleaning procedure stopped working), and for all windows and all wedges. The effect of the pollution on the reflection coefficient is a highly sensitive issue for the DIRC type of detector, and therefore it was studied in great detail. The results are described in Ref. 5.

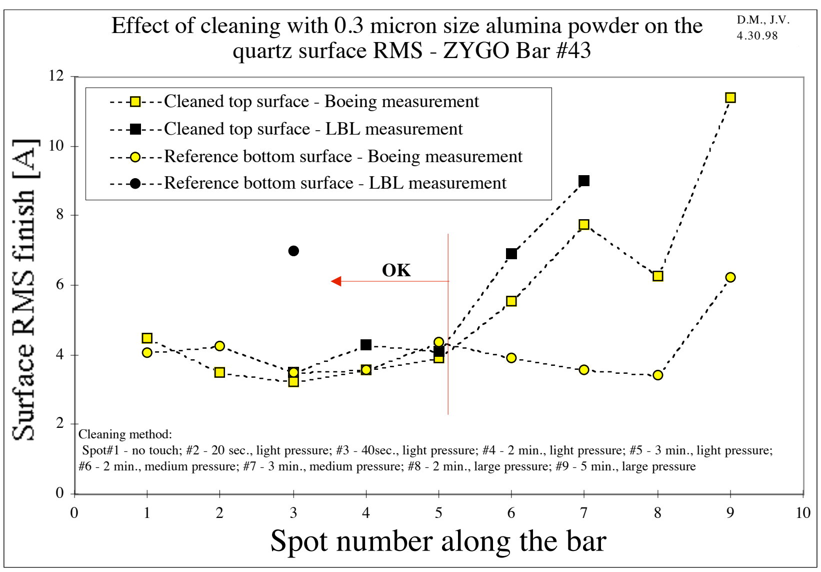

Figure 2. DIRC cleaning method of the quartz surface with the 0.3 μm size alumina powder. The surface rms finish was measured with the ZYGO interferometer at Boeing Co. and at LBL. Cleaning was done by gentle strokes of the surface varying the hand pressure. Method No. 2 was used at the end.

Figure 3 shows the final data from the bar #114, plotted as (1-Reflection coefficient)=f (wavelength), and for bounces off the wide side of the bar. The plotted errors are rms errors based on ten repetitive trials for each intensity component I_i. The systematic errors are harder to evaluate. They depend on many factors, such as surface quality variation, surface pollution (especially in the far UV region), method of the photodiode "peaking" (i.e., finding a spot yielding a consistent maximum reading), dust, background light in the room, surface side choice, lobe effect due to the refraction index variation, etc. To evaluate at least some systematic errors, the measurements were repeated many times, while varying the laser entrance point into the bar, the laser path within the bar, the number of bounces N (by few), avoiding bright spots observed when hitting either a chips or the Nylon supporting buttons, etc. After a lot of practice, I would assign the systematic error of about ±0.0003 to each measurement. Figure 3 also shows three curves based on the scalar reflection

[1] Bar was made from Spectrosil 2000 quartz, Quartz Products Co., 1600 W. Lee St., Louisville, Kentucky 40201, U.S.A. [4]

theory [6], assuming the quartz surface finish of 5, 10 and 15 Å. The internal reflection coefficient is consistent with the surface finish between 6 and 8 Å in the wavelength region between 450 and 650 nm. However, it gets significantly smaller below 350 nm, and its value is no longer consistent with the scalar theory. This discrepancy is not well understood. I have spent a considerable time to check the experimental results at 266 and 325 nm, but I could not find a way to change these values significantly. Figure 3 also shows fit using a polynomial of the fourth order. This fit was used in my spreadsheets, subsequently, to evaluate the DIRC efficiency and mean wavelength response.

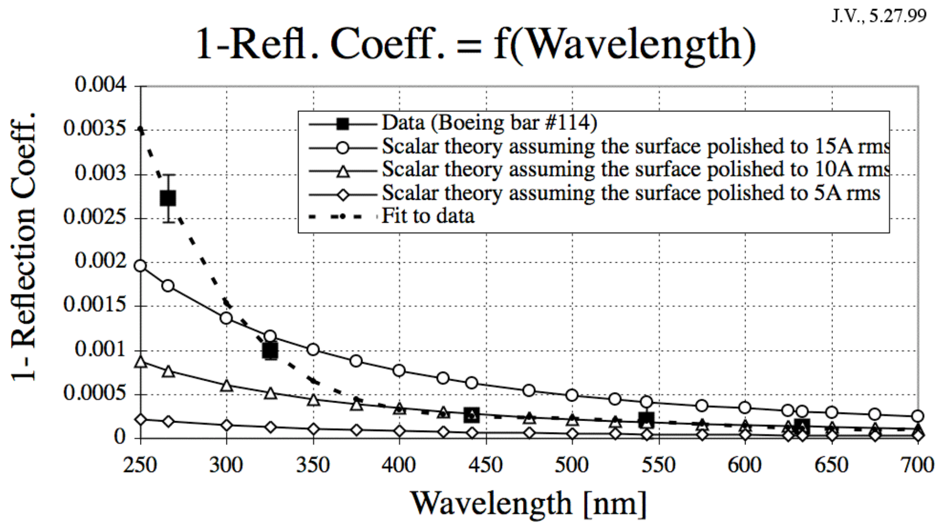

Figure 3. A comparison of the internal reflection coefficient measurements at five different laser wavelengths and the scalar scattering theory, assuming only surface randomness. Data are consistent with ~5-8 Å rms surface finish for wavelengths between 400 and 700 nm. Below ~350 nm, the data does not agree with the simple scattering theory. The laser light bounced from the wide sides of the bar.

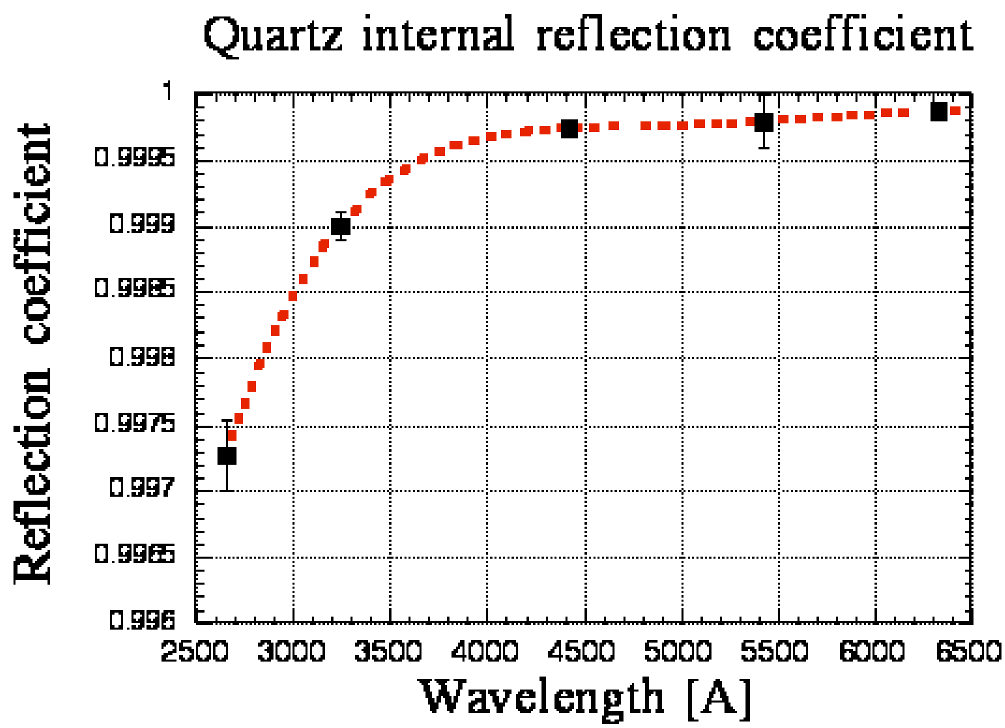

Figure 4. The fifth order polynomial fit to the data of the internal reflection coefficient. The fitted parameters are: $a_0 = 0.93425$, $a_1 = 5.8202 \times 10^{-5}$, $a_2 = -2.0473 \times 10^{-8}$, $a_3 = 3.5575 \times 10^{-12}$, $a_4 = -3.0488 \times 10^{-16}$, and $a_5 = 1.0305 \times 10^{-20}$. The laser light was reflecting from the wide sides of the bar.

2. The wavelength dependence of the DIRC water transmission.

The presented data represent the absolute measurement of the water transmission, i.e., all Fresnel reflection corrections are evaluated.

I learned from the CRID experience, for example, that it is important to measure the water transmission over a distance comparable to an average photon pathlength in the detector. This is necessary to avoid scaling results from a short cell, thus avoiding a propagation of systematic errors. In the case of DIRC, the photon path in water is about ~1.2 m.

The water cell[2] used for this measurement is 1 m long. The use of such a long cell requires lasers, and essentially, excludes the use of monochromators. I have used three laser wavelengths for the water transmission measurement: 266, 325 and 442 nm. The 266 nm wavelength was chosen to probe for possible bacteria contamination. Figure 5 shows the experimental setup (the same setup is also used for the measurement of the internal reflection coefficient).

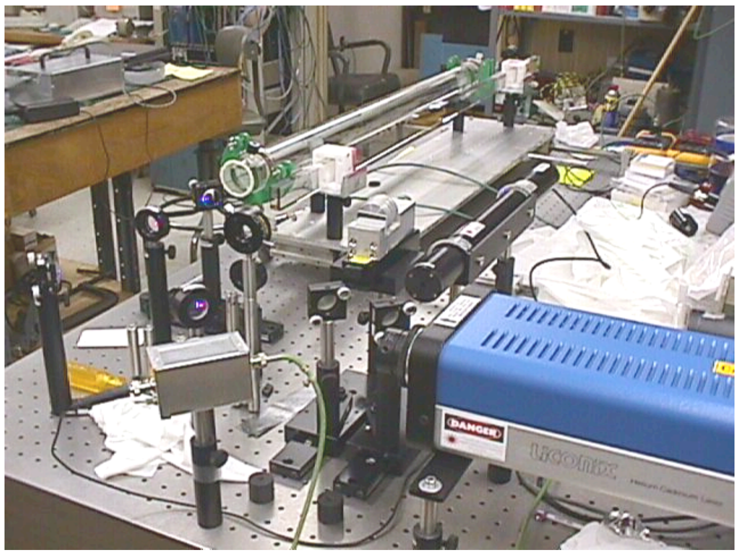

Figure 5. The experimental setup with five lasers used to measure the internal reflection coefficient, and the water transmission in one meter long glass cell.

The measurement is done manually with the help of a spreadsheet, i.e., non-computer control environment. In this test, one needs to measure the transmission of (a) cell empty (obtained by moving the empty cell in and out of the beam), (b) cell full (obtained by moving the full cell in and out of the beam), and (c) a knowledge of the refraction index of water and quartz as a function of wavelength, in order to do the Fresnel corrections. The following equation describes the algorithm:

$$\mathrm{Tr} = \left[\frac{1}{(1-R_{air/quartz})^2}\,\frac{1}{(1-R_{water/quartz})^2}\,\frac{(I_{sample}/I_{ref})\big|_{full\ cell\ in}}{(I_{sample}/I_{ref})\big|_{full\ cell\ out}}\right] \Big/ \left[\frac{1}{(1-R_{air/quartz})^4}\,\frac{(I_{sample}/I_{ref})\big|_{empty\ cell\ in}}{(I_{sample}/I_{ref})\big|_{empty\ cellout}}\right] \qquad (6)$$

Correction factors $R_{water/quartz}$ and $R_{air/quartz}$ are calculated from the wavelength dependent refraction index of each respective medium. To do the measurement correctly, it is necessary to "peak" the photocurrent in each step. The DVM, which measures the photocurrent, is triggered to read a reference diode and a sample diode at the same time. To reduce background from room lights, they are switched off during the measurement. The water sample is brought to the lab in a one-gallon glass bottle. Prior to taking the water sample, the container is rinsed twice in the system's best water (the "SOB supply" water), then it is rinsed twice in the "SOB return" water, before it is taken again for the actual measurement. After the measurement is finished, the cell is drained, the removable cell windows are cleaned by a lint-free

---

[2] A 1 m long, 2 inch diameter, glass water cell was made by a glass shop at University of California, Santa Cruz. The cell has removable windows, which allows a proper cleaning and easy drying. The windows are made of quartz, which is glued with a Hysol glue.

tissue, and the cell is simply let dry by convection in air. The glass container always has some water left over. I leave it in this glass container, even for a period as long as one to two months. The interesting thing is that the bacterial study of this water by the Balaz Water Company showed no growth of bacteria, despite the fact that the similar test indicates a large bacteria count in the SOB return [7]. A possible explanation is that the conditions in the glass bottle do not support the growth of bacteria (it is dark, has no air, has no "food" supply and is relatively cool; in the case of SOB, there is probably a large "food" supply).

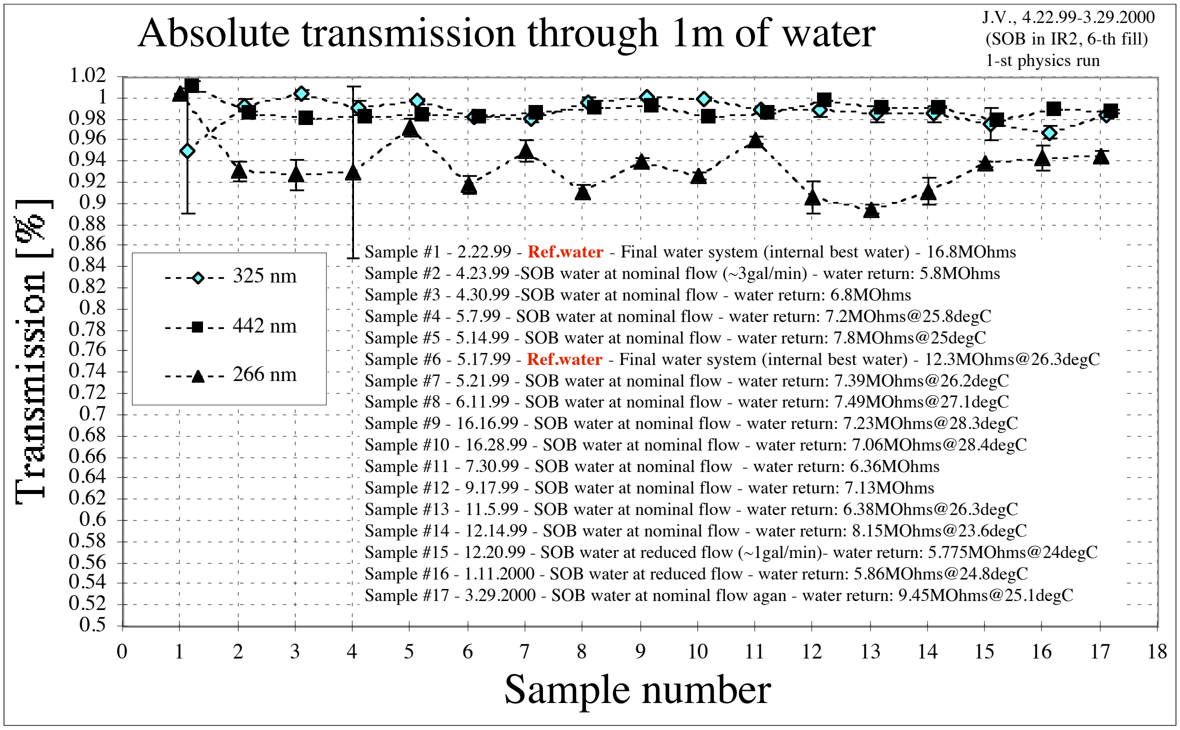

Figure 6. DIRC water transmission measured in a 100 cm long glass cell, and water sample from the SOB return during the first BaBar physics run in 1999-2000. This measurement was done using three lasers.

Figure 6 shows the time history of water transmission measurement during the first BaBar physics run in 1999-2000. The errors shown are rms errors based on three repetitive trials, for a given laser setup. The systematic errors are not shown. The systematic errors are related to effects such as window pollution, dust, water bubbles, the photodiode "peaking," water drying method, bacteria content, a background light in the room, etc. Based on the scatter distribution of data points in Fig. 6, and assuming that the water quality was constant, one could argue that the systematic errors are as much as ±1% at 442 and 325 nm, and perhaps, ±2-3% at 266 nm. The larger systematic error at 266nm was caused by larger intensity instability of this particular laser, which caused errors when "peaking" the photodiode. One can obtain the wavelength dependency of the SOB water return transmission by averaging all measurements in Fig. 6, for each wavelength, during the entire run. The result and the final fit are shown in Fig. 7. This curve was used in the final DIRC efficiency estimate.

The bacteria count in the "SOB return" water, as measured by the Balaz Water Company, was over their maximum count limit during the entire year of operation [7]. This would, for example, cause an emergency shutdown of the water plant at the Intel Company. However, Fig. 7 indicates that the "SOB return" water transmission at 266 nm is not sensitive to it. The wavelength of 266 nm was chosen specifically to be very close to a wavelength where the bacteria's DNA has the highest UV absorption.

As a side comment, one would expect the pollution caused by the EPDM gasket, which is a flexible gasket material sealing the drift boxes in water, to influence the water transmission just below 325 nm (see Fig. 8). There was a great deal of worry about the pollution caused by this gasket, initially, before it was found that one can clean it, for example, by rinsing it in the boiling water. The R&D test results seem to be confirmed because one does not see any obvious effect in this wavelength region in the transmission of water from the "SOB return" water (see Fig. 7).

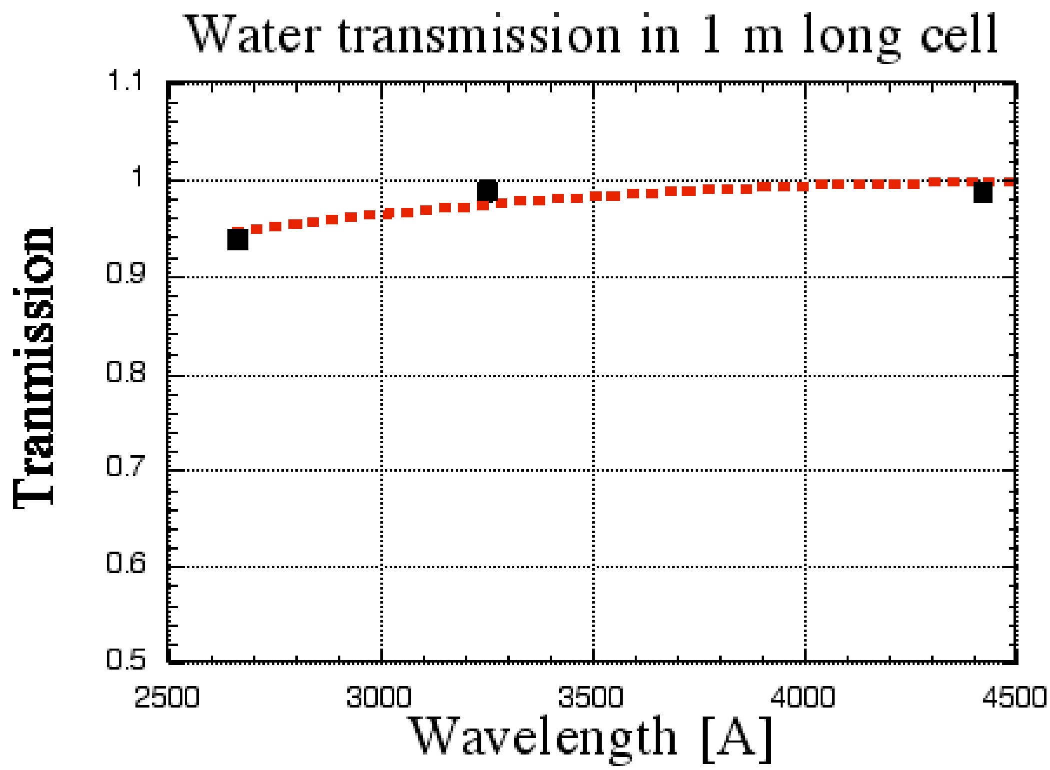

Figure 7. Wavelength dependence of the average DIRC water transmission measured in a 100 cm long glass cell and water sample from the SOB return during the first physics run in 1999-2000. A simple polynomial fit of the third order gave the following parameters: $a_0 = 0.61644$, $a_1 = 0.000200835$, $a_2 = -3.35979 \times 10^{-8}$, and $a_3 = 1.7351 \times 10^{-12}$. This measurement was done using three lasers.

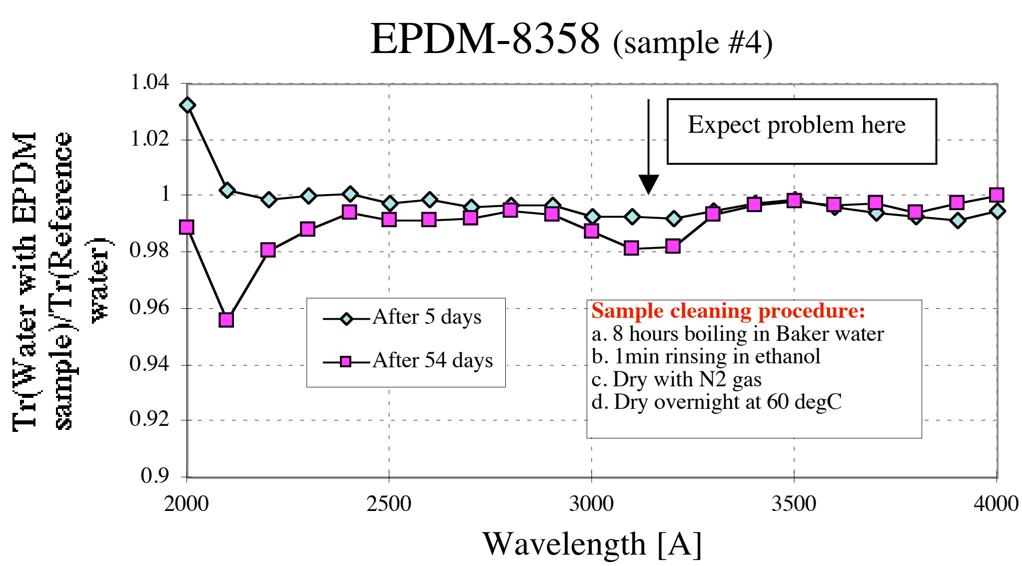

Figure 8. Relative water transmission in the 20 cm long cell (a 1 cm x 1 cm EPDM gasket sample was placed in the water). The sample water is compared to a clean reference water sample. The EPDM sample was cleaned by a procedure described on the figure, and left in a one-gallon glass bottle for 5 or 54 days, while the water was stagnating during this period. This particular measurement was done with a SLAC monochromator and with the help of M. Schneider.

3. The DIRC mirror reflectivity.

Figure 9 shows the DIRC mirror reflectivity as a function of wavelength. My data at three different laser wavelengths (266, 325 and 442 nm) and the manufacturer's data were found to be consistent.

I have done a few additional measurements to check that the mirror reflectivity does not depend on some other variable. Dependencies such as (a) the laser beam angle of incidence relative to the mirror plane, (b) the laser beam polarization orientation, or (c) possible interference effects in air coupling between the mirror and the end of the quartz bar (this simulates the real end of the DIRC bar to the mirror). Figure 10 shows the experimental setup to understand the various Fresnel reflection corrections involved. Figures 11-13 show that there are no hidden surprises at a level of <5%, and therefore, I used the Company's data [8] in my spreadsheet calculations.

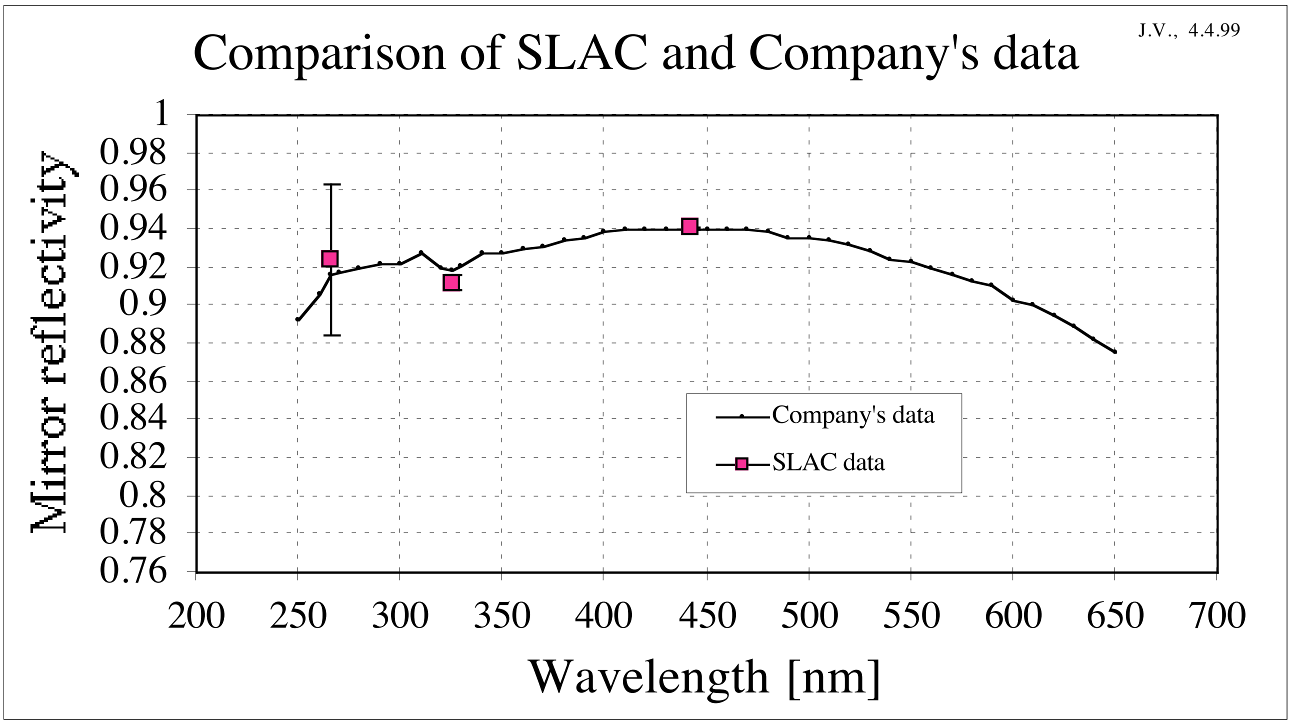

Figure 9. DIRC mirror reflectivity as a function of wavelength. My data is measured with a laser, the mirror is in air, the laser beam is perpendicular to the mirror, and it is polarized vertically. The mirror manufacturer's data are measured with the monochromator [8] (their data arrived after my measurement was finished).

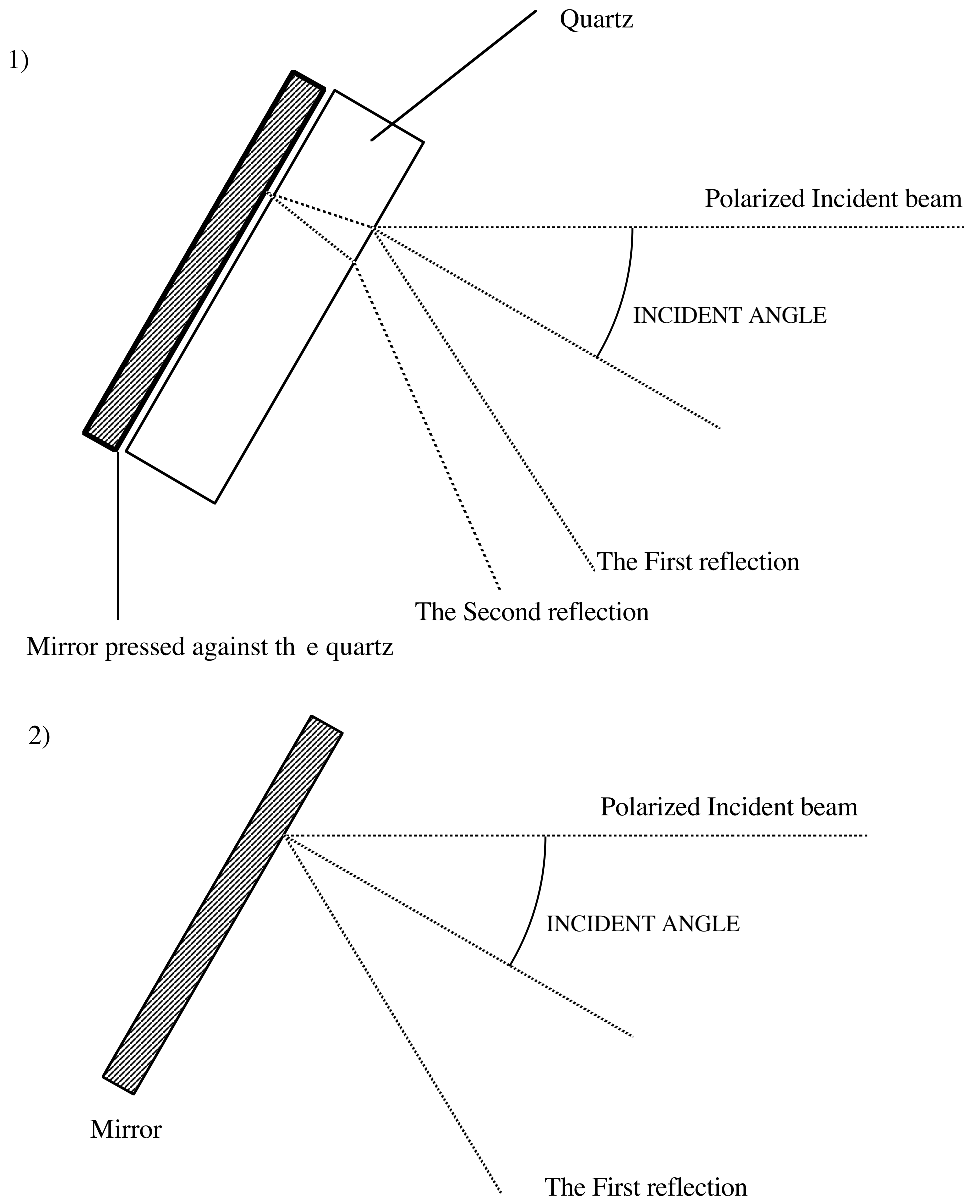

Figure 10. Experimental setup to measure the DIRC mirror reflectivity under two conditions: (1) with a quartz bar pressing against the mirror to simulate the real DIRC conditions, and (2) with the mirror alone. The light polarization from the laser is vertical (500:1), and it can be rotated optically into the horizontal plane. The DIRC mirror is front coated.

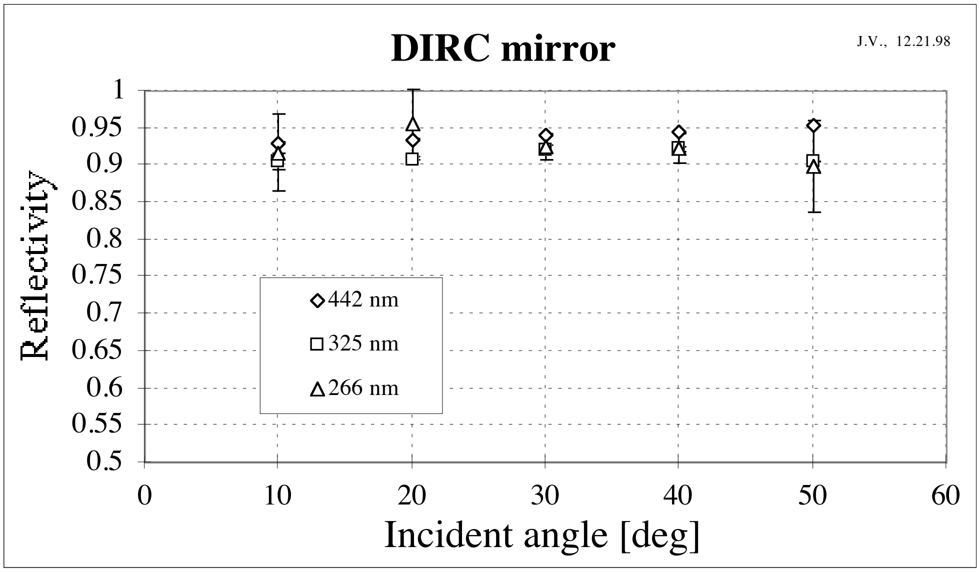

Figure 11. DIRC mirror reflectivity as a function of incident angle, or different wavelengths. The data is measured with a laser, the mirror is in air, and the laser beam is polarized in vertical direction (see Fig. 10 for explanation). The laser polarization is vertical and better than 500:1 (laser was Lyconix 4214NB).

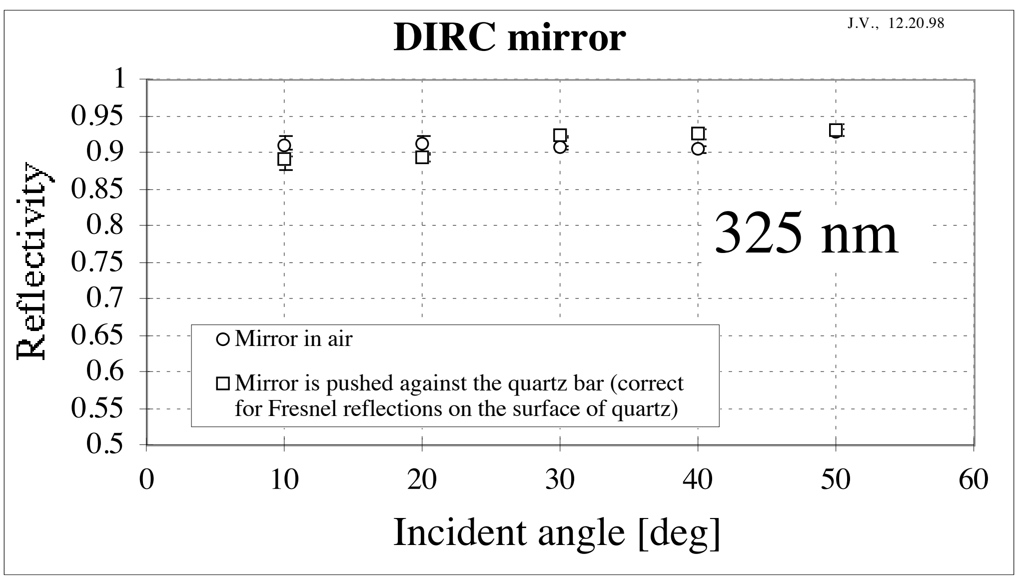

Figure 12. DIRC mirror reflectivity as a function of incident angle at 325 nm. The data is measured with a laser, the mirror is either in air (circles), or is pushed against a polished quartz bar with air coupling, and with appropriate Fresnel corrections (squares) (see Fig. 10 for explanation). The laser polarization was vertical and better than 500:1 (laser was Lyconix 4214NB).

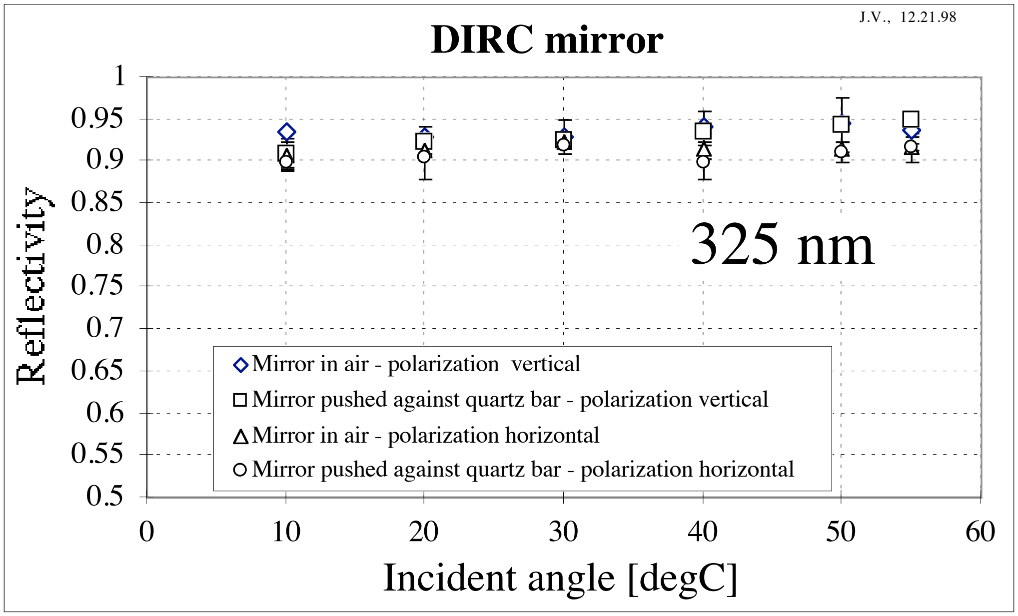

Figure 13. DIRC mirror reflectivity as a function of incident angle at 325 nm. The data is measured with a laser with two polarization orientations; the mirror is either in air, or is pushed against polished quartz bar with air coupling, and with appropriate Fresnel corrections (see Fig. 10 for explanation).

The quartz bars have to be supported within the bar box. The idea is to choose such a material, which minimizes the reflection loss when a photon reflects from it. Figure 14 indicates that, for example the Nylon creates very large reflection losses. This is true for all soft plastic materials such as Teflon or Rubber. The harder plastic materials, such as Kapton or Mylar, perform better. Metals, such as Aluminum, perform even better. Fig. 14 indicates that the reflectivity of any material depends on the pressure with which the material is pressed against the quartz bar. To quantify this better, we constructed a press (see Fig. 15), which was calibrated to express the force per area in the psi units. Figure 16 shows the reflection losses in Aluminum shim foils as a function of the load. One can see that the loss is less than 1% for typical practical loads. For comparison, Fig. 17 shows that the uncoated Kapton or Mylar shims would be a worse choice. Figure 18 shows also that the mirror reflectivity does not change much as a function of the load. Based on these tests, DIRC has chosen the Aluminum as a material for shims between the bars, and Nylon for the supporting buttons.

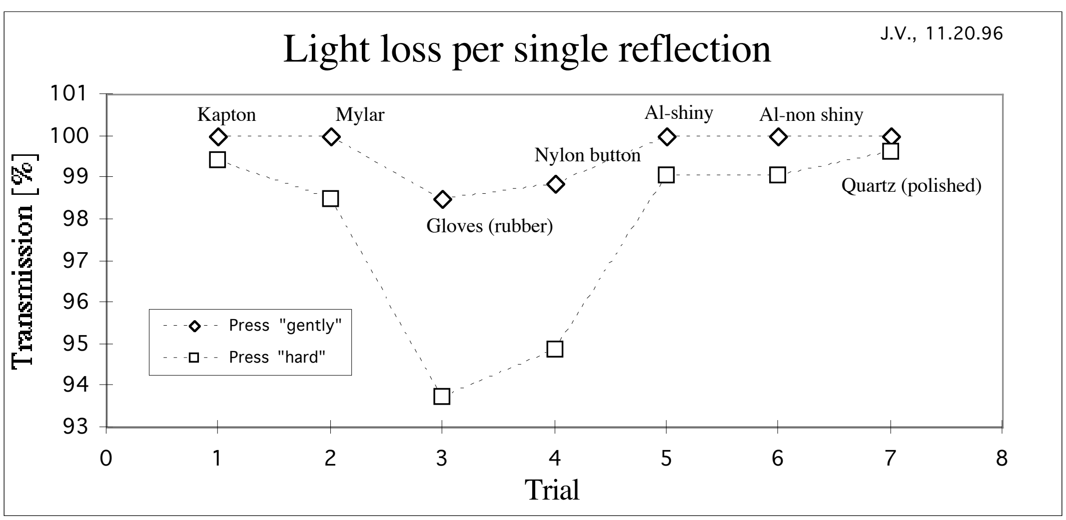

Figure 14. A single bounce reflection loss from various materials attached to the bar at a place of reflection. This result motivated a construction of the press to quantify the results by knowing the load on the shim (the press is shown in Fig. 15).

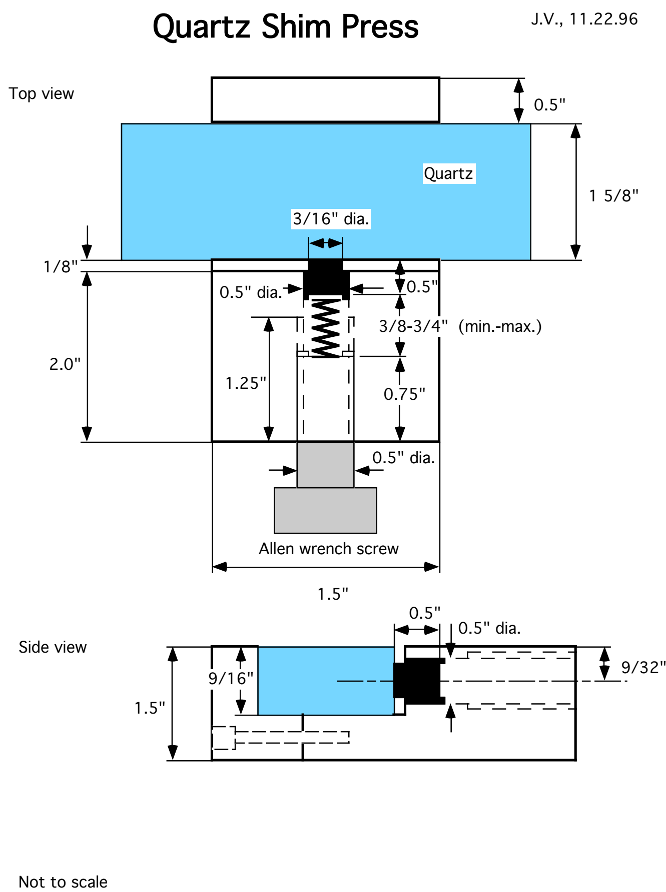

Figure 15. A press to create the known force on the shim material when pressing against the quartz bar surface.

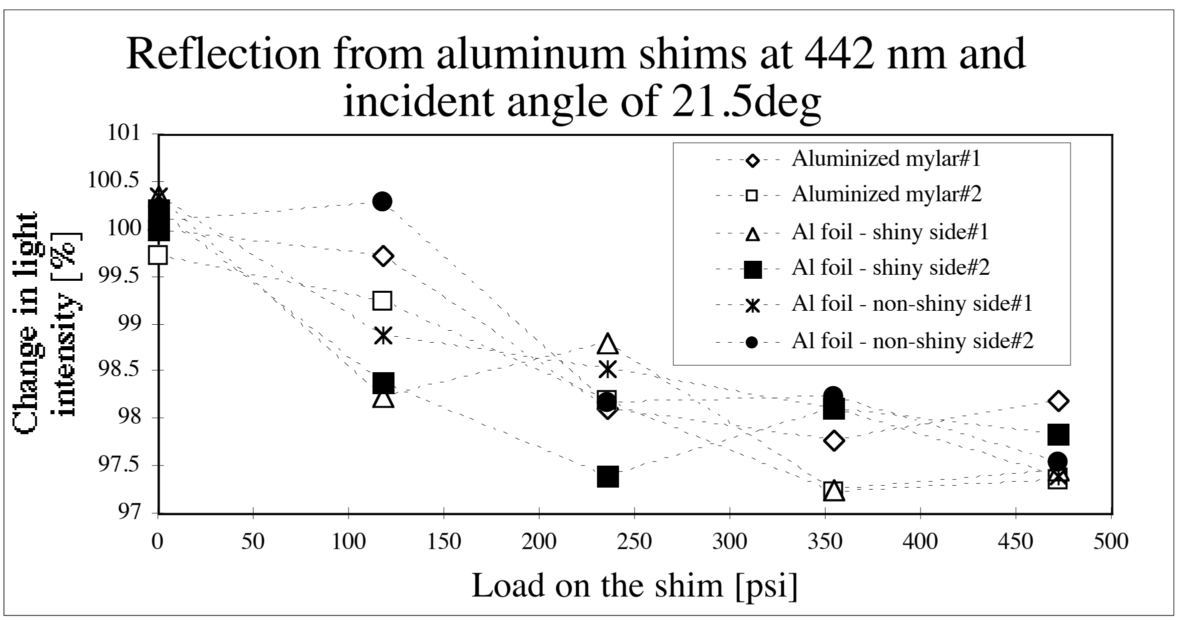

Figure 16. A single bounce reflection loss from the aluminum shims attached to the bar at a point of reflection. We used the non-shiny the aluminum shims to separate the bars in DIRC; their thickness was produced by etching.

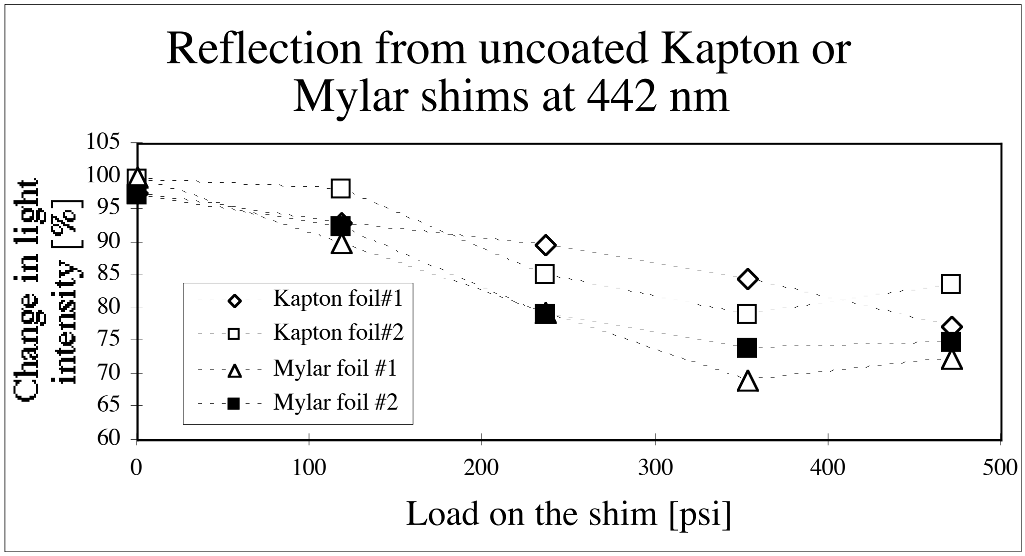

Figure 17. A single bounce reflection loss from uncoated Kapton or Mylar foils attached to the bar at a point of reflection. The incident angle is 21.5º.

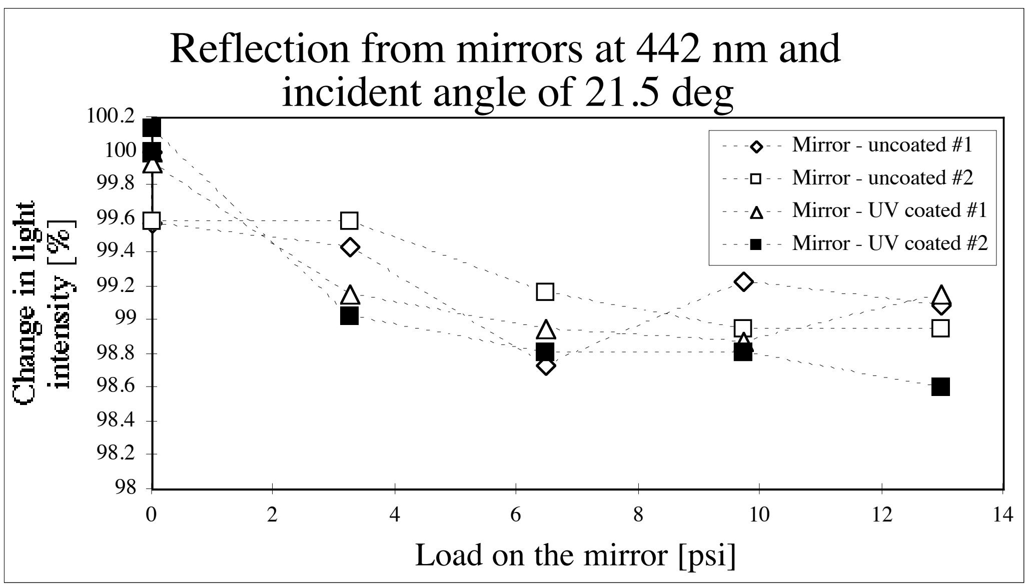

Figure 18. A single bounce reflection loss from the mirrors as a function of load.

4. The refraction index of water, quartz and EPOTEK 301-2 glue.

To make various corrections throughout this paper, for example such as calculated in equation (6), it is necessary to know the refraction index of water, quartz and EPOTEK 301-2 optical glue used for gluing bars. Figures 19 and 20 show the refraction index of quartz [9] and water [10]. Figure 21 shows the calculated reflection coefficients at incidence angle of 0º for the boundaries of quartz/water and quartz/EPOTEK 301-2 [11].

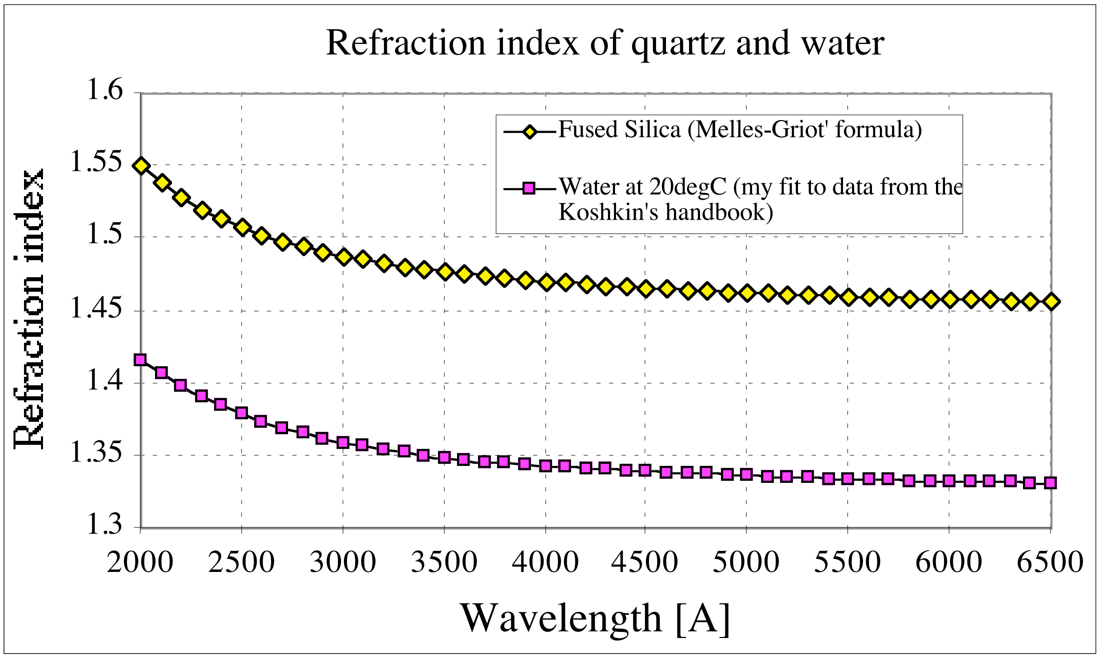

Figure 19. A wavelength dependence of the refraction index (water and quartz) [9,10].

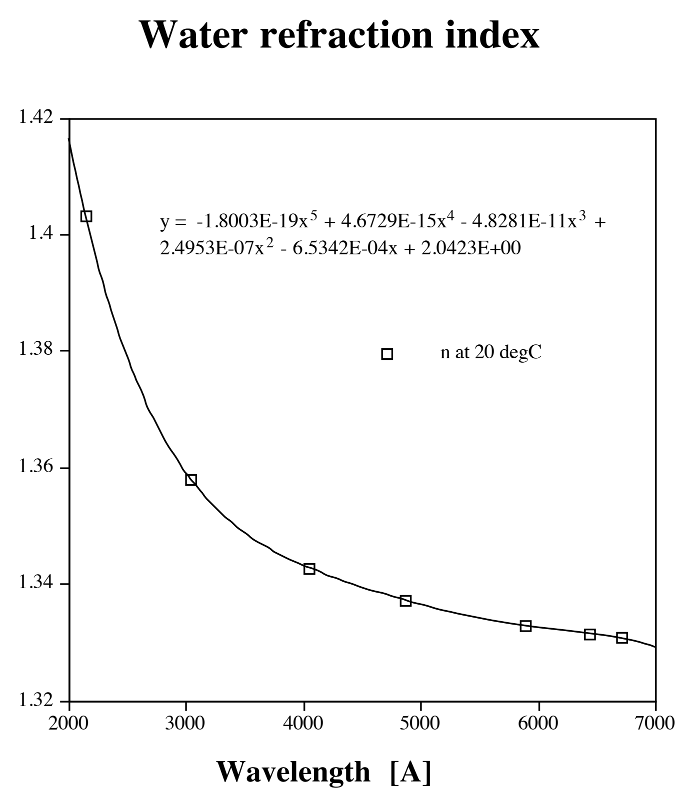

Figure 20. The author’s simple polynomial fit to the water refraction data of Ref. 10.

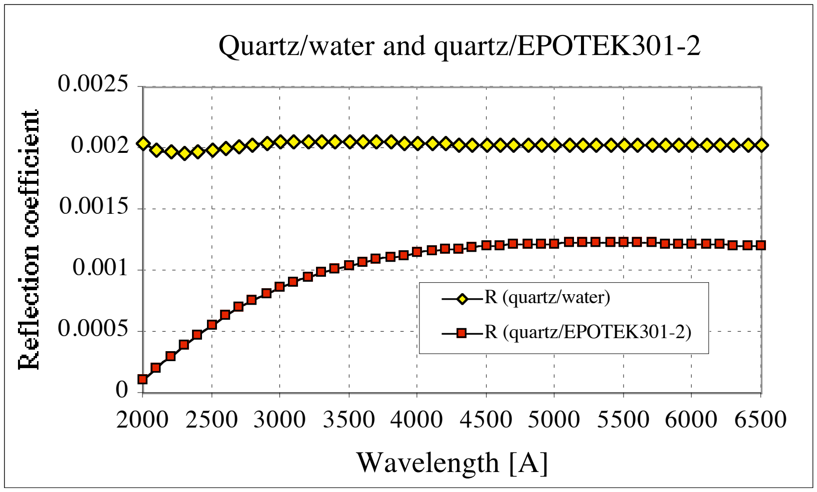

Figure 21. Wavelength dependence of the reflection coefficients at incidence angle of 0º for quartz and water, and quartz and EPOTEK301-2 interfaces due to mismatches of the refraction index. Notice that the water/quartz reflection coefficient is almost independent of wavelength.

5. No, Npe and the mean refraction index dependence on the track dip angle.

A number of photon internal reflection bounces depends on the dip angle of the track. Because of the chromatic dependency of the internal reflection coefficient (see Figs. 3 and 4), and to a lesser degree other chromatic dependencies, one would expect that the mean Cherenkov angle is a function of the dip angle. To estimate this effect, it is necessary to take into account all efficiencies involved. In this note, this was done for three track angles of incidence relative to the quartz bar: 0º, +60º, and –60º. Figure 22 shows the final efficiency obtained for a 0º incident angle, i.e., for a case where the track is perpendicular to the quartz bar.

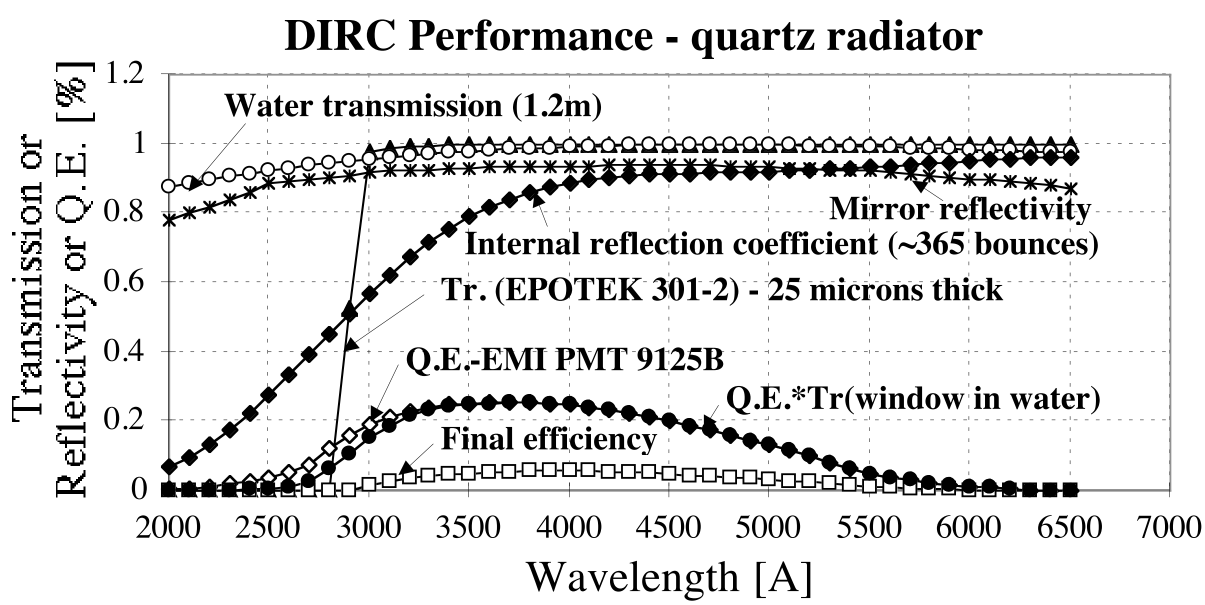

Figure 22. DIRC performance for a track perpendicular to the quartz bar in the middle of the BaBar sensitive area: quantum efficiency of EMI9125B PM, transmission of one glue joint 25 μm thick made with EPOTEK 301-2 optical epoxy, water transmission in 1.2 m long path, mirror reflectivity, the internal reflection coefficient assuming ~365 bounces on average, and the DIRC final efficiency taking into account other correction factors.

A number of detected photoelectrons N_{pe} is calculated in this note as follows:

$$N_{pe} = L \frac{z^2 \alpha}{\hbar c} \int_{E_1}^{E_2} \prod_i \varepsilon_i(E) \sin^2 \theta_c(E)\, dE \quad , \tag{7}$$

where a product $\Pi\varepsilon_I$ is the empirically determined quantity, and E_1 and E_2 define the bandwidth of the device. Clearly, only non-chromatic constants can be simply factored out of the integral in equation (8). N_o of the device is defined as:

$$N_o = \frac{z^2 \alpha}{\hbar c} \int_{E_1}^{E_2} \prod_i \varepsilon_i(E)\, dE \quad , \tag{8}$$

and one can approximate the number of photoelectrons with a usual formula Npe ~ N_o L $\sin^2 \langle\Theta_c\rangle$, where $\langle\Theta_c\rangle$ is the average Cherenkov angle. This angle can be determined from the average wavelength obtained from the distribution of the "final efficiency" shown in Fig. 22, which in turn determines the average refraction index. However, in this note, I am actually using equation (8) to determine Npe, i.e., the final numbers are derived from the numerical integration of various chromatic dependencies, scaled by several wavelength independent factors. The wavelength dependent factors, which cannot be pulled out of the integral, are:

(a) PMT quantum efficiency (manufacturer's data; see Fig. 22),

(b) Transmission of PMT window in water (manufacturer's data; see Fig. 22),

(c) EPOTEK 301-2 transmission (manufacturer's data and the SLAC measurement; see Fig. 22),

(d) Reflection coefficients on the boundary of quartz and water and quartz and EPOTEK302-1 interfaces (my estimate based on the manufacturer supplied data; see Section 4),

(e) Internal reflection coefficient after N bounces (my measurement, see Section 1; in the spreadsheet calculation, I estimate the average number of bounces N to be ~365 at 0°, ~145 at +60° and ~70 at –60° incident angle),

(f) Quartz transmission (I use J. Schwiening's measurement [2] of the attenuation length of λ = 499.5±167 m at 442 nm, and then I scale it to other wavelengths according to a $1/\lambda^4$ law),

(g) Water transmission (my measurement; see Section 2), and

(h) Mirror reflectivity (my measurement; see Section 3).

The wavelength independent factors are:

(a) PMT packing fraction (I estimate ~0.52, which includes a factor of 1.2 for the light catcher effect, the PMT packing fraction, and the gaps between the SOB sectors),

(b) Fraction of photons exiting the quartz into the photon detector (I used ~0.60-0.62; this is the only number, which I have "borrowed" from the Monte Carlo [12]),

(c) Electronics detection efficiency (I use, rather arbitrarily, a factor of ~0.9 at the moment. When and if the final average detection efficiency is known (an attempt to do it using the "pedestal" mode failed), one can simply scale the results in Table 1 appropriately), and

(d) Photon reflection losses when hitting the Nylon buttons or Aluminum shims (neglected in this note).

Table 1 summarizes the results of the spreadsheet calculation for all three angles of incidence and a β = 1 particle. One can see that at 0° incident angle the average wavelength is about 3979.27 Å, the average refraction index of the fused silica quartz is 1.470344, the expected number of photoelectrons Npe is ~28, and N_o is ~31 cm^{-1}. The average wavelength was obtained by a numerical integration of the final efficiency shown in Fig. 22.

Running the same spreadsheet for two other incident angles of +60º and –60º, I find that the average wavelength, as obtained from the final efficiency distribution, changes slightly. The maximum shift is less than ~8 nm, which would result in a change of the refraction index of only $\Delta n/n \sim 0.0008/1.470344 \sim 0.00054$. Such shift would have negligible effect on the timing resolution of ~1.6 ns of the present DIRC PMT (in fact, it would be even acceptable for a PMT with ~100 ps intrinsic resolution because the timing shift is less than 20 ps). The average Cherenkov angle (for β = 1 particles) shifts only by ~0.5 mrad, which may contribute slightly to the systematic error of the DIRC analysis. While the average N_o changes by only ~30%, the number of photoelectrons changes by more than a factor of two as a function of dip angle; this is because it is mainly driven by a change in the path length through the quartz bar. The error on the absolute value of Npe is at least ±10-20% at present.

Table1

Incident angle	Npe	Average wavelength [Å]	Average θ_c (β=1) [mrad]	Average n	N_o [cm^{-1}]
0º	28	3979.27	822.94	1.470344	31
+60º (toward mirror)	64	3934.81	823.26	1.470846	35
-60º (toward PMT)	73	3905.25	823.47	1.471190	40

Conclusions.

1. This paper presents the measurement of wavelength dependency of the absolute value of the internal reflection coefficient. To my knowledge, this is the best measurement of this dependency ever made.
2. This paper also presents the transmission measurement of the SOB water during the first year of running BaBar. There is no obvious sign of the water pollution due to the EPDM gasket, which was our initial worry. There is also no deterioration of the water transmission due to a relatively high-bacteria content in the SOB water return at small wavelengths.
3. This paper presents the measurement of the mirror reflectivity as a function of the wavelength, the angle of incidence, and under a condition when mirror presses against the polished bar surface, as is the case in DIRC.
4. This paper presents the expected number of photoelectrons Npe and N_o for three incident angles: 0º, +60º, and –60º.
5. This paper also estimates the average shift in the mean Cherenkov angle and the refraction index as a function of three track dip angles: 0º, +60º, and –60º.
6. B. Ratcliff's original estimate of the expected number of photons, based on much less knowledge of the final DIRC parameters, such as the internal reflection coefficient, turned out to be actually reasonably good [13].

Acknowledgement.

I would like to thank Bob Reif for making a movable table for the water cell and quartz bar setup. I also thank Michael Schneider for suggesting to make the 1 m long water glass cell in the UC Santa Cruz glass shop, and for helping with a couple of measurements using his monochromator (the EPDM gasket water pollution and EPOTEK 301-2 glue transmission).

References.

1. H. Krueger, M. Schneider, R. Reif and J. Va'vra, BaBar DIRC Note #18, January 5, 1996.
2. H. Krueger, R. Reif, X. Sarazin, J. Schwiening and J. Va'vra, BaBar DIRC Note #40, May 20, 1996.
3. J. Cohen-Tanugi, M. Convery, J. Schwiening and J. Va'vra, BaBar DIRC Note #122, April 19, 1999.
4. M. Convery, B. Ratcliff, J. Schwiening and J. Va'vra, BaBar DIRC Note #130, April, 2000.
5. J. Cohen-Tanugi, M. Convery, J. Schwiening and J. Va'vra, BaBar DIRC Note #131, April, 2000.
6. J. M. Elson, H. E. Bennett, and J. M. Bennett, Scattering from Optical Surfaces, Applied Optics and Optical Engineering, Vol. VII, Chapter 7, Academic Press, Inc., ISBN 0-12-408607-1979.
7. J. Va'vra, BaBar DIRC Hypernews #700 and #752, December 1999.
8. The DIRC mirrors were manufactured by the United Lens Company, Las Vegas, NV.

9. This parameterization of the quartz refraction index comes from the Melles-Griot Company's catalog.

10. The refraction index data come from N.I. Koshkin, M.G. Shirkevich, Handbook of Elementary Physics, 1982.

11. The EPOTEK Company provided data of refraction index of EPOTEK 301-2 optical glue at 589.3 nm (a sodium D line) and few wavelengths in the range of 1000-5000nm. Author extrapolated these values into the DIRC range.

12. P. Coyle, H. Kawahara, A. Lu, G. Lynch, G. Mueller, D. Muller, B. Ratcliff, and C. Simopoulos, Nucl. Instr. & Meth. A343 (1994) 292.

13. B. Ratcliff, SLAC-PUB-6047, January 1993.